An ab Initio Study of the Three-Channel Reaction between Methanol and Hydrogen Atoms: BAC-MP4 and Gaussian-2 Calculations

G. Lendvay,* T. Bérces, and F. Márta

Central Research Institute for Chemistry, Hungarian Academy of Sciences, P.O. Box 17, H-1525 Budapest, Hungary

Received: October 14, 1996[⊗]

Rate coefficients for the three-channel reaction of methanol with H atoms were calculated from ab initio saddle point properties using conventional transition state theory. The saddle point geometries and energies were determined using the BAC-MP4 and the Gaussian-2 methods. The (classical) ab initio barrier heights for the formation of CH_2OH, CH_3O, and CH_3 are 11.3, 16.3, and 30.5 kcal mol^{-1}, respectively, as obtained using the BAC-MP4 method, and 10.6, 16.3, and 25.6 kcal mol^{-1}, respectively, from Gaussian-2 calculations. The rate coefficients obtained from the G-2 calculations are 2.0×10^{-16}, 1.9×10^{-20}, and 1.9×10^{-28} cm^3 molecule^{-1} s^{-1} at 298 K. The BAC-MP4 rate coefficient at 298 K is similar for channel 2 and lower than the G2 rate coefficient of the overall reaction agrees, within a factor of 2, with the recommendation of Tsang in a broad temperature range. Its temperature dependence is represented by $k = (1.57 \pm 0.56) \times 10^{-15} T^{1.70\pm0.05}$ exp(-2735 ± 23 K/T) cm^3 molecule^{-1} s^{-1}. Theory suggests that formation of CH_2OH is the dominant channel, contributing to the overall reaction by over 95% below 1200 K and by about 90% at 2000 K. The formation of $CH_3 + H_2O$, which is the most exothermic channel, is unimportant in the whole temperature range studied.

I. Introduction

Methanol is considered a potential substitute for gasoline,[1] mainly because its combustion causes less air pollution than that of gasoline: the emission of pollutants CO, NO_x, hydrocarbons, and soot is significantly lower.

The understanding of the mechanism of methanol combustion requires the knowledge of the kinetics of the contributing elementary reactions. A chemical kinetic data base for reactions participating in methanol combustion has been published by Tsang,[2] and a critical review has been presented recently by Grotheer et al.[3] It appears from these compilations that the reaction of H, OH, and O with CH_3OH is responsible for most of the CH_3OH consumption in methanol combustion and flame. The reaction with OH radical is predominant in lean and moderately rich methanol flames, while the reaction with H atoms accounts for about 53% of CH_3OH consumption under fuel rich conditions.[3] Despite their importance, the kinetics of some of these reactions and especially the branching ratios for the different product channels are not very well-known. This is particularly true for the H + CH_3OH reaction where experimental study is made difficult by the fact that three different reactive species can be formed in reaction channels corresponding to hydrogen atom attack at three different sites of the methanol molecule:

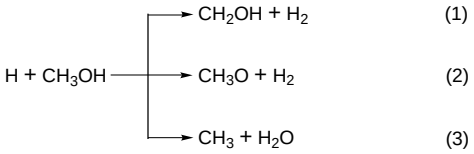

(1)
(2)
(3)

Since these products are characterized by different reactivities and are expected to have different fates in the combustion system, it is of primary importance to establish reliable values for the branching ratios.

Information available in the literature on the branching ratios of reactions 1−3 is scarce and contradictory. Following the suggestion of Aders and Wagner,[4] it was assumed in the early papers that reaction 3, forming CH_3 radical, is faster than the H atom abstraction reactions 1 and 2. Later, however, it was shown in a study of methanol pyrolysis[5] and confirmed in direct experiments[6,7] that the ratio of the rate of CH_3 formation and H atom abstraction is between about 10 and 30.

Early modeling involving the reaction of hydrogen atoms with methanol made no distinction between hydrogen abstraction from the OH or the CH_3 groups of methanol. It is only recently that CH_2OH and CH_3O are treated as different species in modeling studies. It is now recognized that CH_2OH is the dominant product of the reaction of H atoms with methanol at low temperatures[8] and that the CH_2OH/CH_3O ratio changes with temperature.

As the experiments were not able to determine firmly the branching ratios for the product formation so far, theoretical studies seem to be necessary. In order to learn more about the kinetics of the site-specific reactions between hydrogen atom and methanol, we have undertaken the theoretical investigation of reactions 1−3. Ab initio calculations were performed for all reactants, products, and transition structures, and the rates for the three reaction channels were obtained by applying transition state theory. High-quality ab initio techniques were used, namely the BAC-MP4 method[9−11] (bond additivity correction of MP4 calculations) proposed by Melius and coworkers and the Gaussian-2 method[12−15] of Pople and coworkers. Thus, the comparison of the performance of the two methods became possible.

The paper is organized as follows: First the ab initio techniques are reviewed briefly. The results of the geometries and energetics are presented in parts A and B of section III, respectively. The rate coefficients for the overall reaction and for the individual channels are presented and compared with experiment in section III.C. A brief summary of the calculated isotope effects is given in section III.D.

II. Technical Details

The geometries, vibrational frequencies, and energies of the reactants, transition structures, and products were calculated by

[⊗] Abstract published in *Advance ACS Abstracts,* January 15, 1997.

S1089-5639(96)03188-X CCC: $14.00

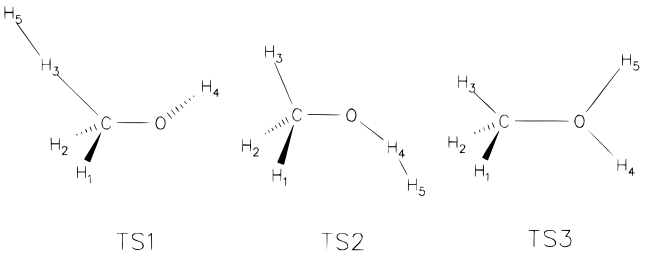

Figure 1. Transition structures for reactions 1−3.

the BAC-MP4[9−11] and the Gaussian-2[12−15] methods. The ab initio calculations were performed with the Gaussian-92[16] and the HONDO-8[17] suites of programs. The BAC-MP4 corrections were obtained with our own code. Rate coefficients were determined by conventional transition state theory[18] including Wigner tunneling corrections.[19] In the TST calculations internal rotors were approximated as low-frequency vibrations.

III. Results and Discussion

A. Properties of the Transition Structures. *Geometries*. The transition structures TS1, TS2, and TS3 of reactions 1−3, respectively, are displayed in Figure 1. The optimized geometries are given in Table 1.

In the TS of channel 1, where the H atom is abstracted from the methyl group of methanol, the H−H−C link is close to linear. The length of the breaking C−H bond is about 1.35 and 1.37 Å according to the HF and MP2 calculations, respectively. Both are significantly larger than the bond length in methanol, being 1.081 (HF) and 1.090 Å (MP2). The length of the forming H−H bond is 0.96 and 0.93 Å as obtained from the HF and the MP2 calculations, respectively, also longer by about 0.2 Å than the H−H distance in the product H_2 molecule. Comparing the transition structures obtained at different ab initio levels, one can observe that the HF geometry is somewhat less product-like than the MP2 structure.

The transition structure of channel 2 is characterized by a slightly bent O−H−H link, with an OH distance of 1.16 and 1.25 Å and H−H distance of 0.95 and 0.87 Å as obtained at the HF and MP2 level, respectively. In this case, the HF structure is again a little less product-like than the MP2 geometry.

At the saddle point of channel 3, in which water is formed, the C−O bond length is increased compared to that in methanol. In this case, the MP2 structure is tighter, since both the C−O and the O−H_5 bond lengths are smaller than in the UHF geometry. It cannot be decided unambiguously whether the HF or the MP2 structure resembles more the products or the reactants. As a conclusion, in this set of reactions the HF geometries are more reactant-like as compared to the MP2 structures if H atom abstraction takes place (as in channels 1 and 2), but no such distinction can be made in the case of channel 3. The relative location of the HF and MP2 saddle points shows no obvious relation to the reaction heat (listed in Table 7).

Bond Orders in the Transition Structures. The location of the transition structures, i.e., the question whether they represent early or late barriers, cannot be easily judged alone from investigation of the geometries only. The study of bond orders, calculated from ab initio wave functions,[20−23] enables one to answer such questions. The value of the bond order indices may be used as a measure of the degree of the development of a bond.[22−27] The calculation of such indices is very quick and informative.[21−25] As discussed in refs 22 and 23, the most practical way of getting reasonable bond order and valence indices is to calculate them from the UHF/STO-3G wave function. The values one obtains are not the integer numbers of elementary chemistry but are very close to them. The valence of carbon is between 3.97 and 3.99; that of H atoms varies between 0.95 and 0.97 in all the structures reported. The bond order and free valence indices in the transition structures for reactions 1−3 obtained at both the HF and the MP2 geometries are collected in Table 2. At the UHF geometry of TS1, the bond order of the breaking C−H bond is 0.42; that of the forming H−H bond is similar, 0.50. This indicates that the reaction is about halfway between the reactants and the products, being a little closer to the latter. The transition structure of channel 2 is more product-like than that of channel 1, as by this point along the minimum energy path the bond order of the O−H bond decreases to 0.39 and that of the H−H bond develops to 0.53. The MP2 structure is definitely more product-like both in TS1 and in TS2. The expectation that an exothermic reaction has a reactant-like saddle point is not fulfilled, but the

TABLE 1: Bond Lengths and Bond Angles of the Transition Structures for Channels 1−3

	TS1		TS2		TS3	
	HF	MP2	HF	MP2	HF	MP2
			Bond Lengths (Å)			
C−O	1.371	1.389	1.412	1.401	1.783	1.701
C−H_1	1.084	1.097	1.084	1.095	1.076	1.086
C−H_2	1.078	1.087	1.085	1.096	1.076	1.086
C−H_3	1.351	1.373	1.084	1.096	1.074	1.083
O−H_4	0.947	0.971	1.160	1.249	0.953	0.982
H_3−H_5	0.959	0.927				
H_4−H_5			0.867	0.867		
O−H_5					1.337	1.213
			Bond Angles (deg)			
H_1−C−O	115.1	115.5	111.0	111.5	105.9	107.1
H_2−C−O	110.1	109.3	112.0	112.6	105.9	107.1
H_3−C−O	110.1	110.6	106.8	106.1	100.4	100.9
C−O−H_4	110.1	110.6	106.8	106.5	100.4	104.2
C−H_3−H_5	177.0	178.2				
O−H_4−H_5			173.2	171.2		
C−O−H_5					166.0	156.6
			Dihedral Angles (deg)			
H_1−C−O−H_4	177.5	174.6	−62.6	−63.3	−61.9	−61.3
H_2−C−O−H_4	48.2	45.1	62.3	60.0	61.9	61.4
H_3−C−O−H_4	68.6	71.8	179.0	178.9	180.0	180.0
H_5−H_3−C−O	1.9	2.3				
H_5−H_4−O−C			179.6	0.0	0.0	0.0

TABLE 2: Bond Orders and Free Valences on Selected Atoms in the Transition Structures for Reactions 1−3[a]

	TS1		TS2		TS3	
	HF	MP2	HF	MP2	HF	MP2
			Bond Orders			
C−O	1.06	1.07	1.01	1.01	0.41	0.43
$C-H_1$	0.97	0.97	0.97	0.97	0.98	0.98
$C-H_2$	0.97	0.97	0.97	0.97	0.98	0.98
$C-H_3$	0.42	0.36	0.97	0.97	0.98	0.98
$O-H_4$	0.93	0.94	0.39	0.22	0.95	0.96
H_3-H_5	0.50	0.56	0.00	0.00	0.00	0.00
H_4-H_5	0.00	0.00	0.53	0.73	0.00	0.00
$O-H_5$	0.00	0.00	0.00	0.00	0.46	0.60
			Free Valences			
C	0.42	0.36	0.0	0.0	0.53	0.50
O	0.0	0.0	0.49	0.68	0.23	0.13
H_3	0.07	0.07	0.0	0.0	0.0	0.0
H_4	0.0	0.0	0.07	0.04	0.0	0.0
H_5	0.35	0.29	0.31	0.13	0.48	0.31

[a] The calculations were done at the UHF/STO-3G level[22] at the HF and MP2 geometries, respectively.

tendency is that the transition state is earlier in the exothermic reaction 1 than in the thermoneutral reaction 2.

The interatomic distances in the HF transition structure of channel 3 are very large. Because of this the C−O and O−H bond orders are small. In the tighter MP2 structure the bond orders are higher, 0.43 and 0.60 for the C−O and $O-H_5$ bonds, respectively. The extension of the C−O and the O−H bonds as compared to the corresponding single bonds in the reactant and product, respectively, is, however, similar; both are about 0.27 Å. The large difference between the bond orders of the O−H bond and the C−O bond seems to be exaggerated. The reason is probably that at this tight geometry the wave function is such that the total valence of the O atom is higher than it is generally (2.13 instead of 2), and this accounts for the too high bond orders of the bonds of the O atom.

The investigation of the free valences of the atoms at the reactive center leads to conclusions that are very similar to those obtained from the bond order considerations. The free valence characterizes the free radical nature of an atom in the molecule. For example, at the HF geometry of TS2, the free valence of the O atom is 0.49 while that of H_5 is 0.31, indicating that CH_3O is far from being a free radical (an early stage of the reaction). The attacking H atom does have a free radical nature which is delocalized between the atoms of the forming H_2 molecule. At the more product-like MP2 geometry, the fragments are much less connected and the CH_3O fragment has greater free radical character (the free valence on O is 0.68) while the H_2 fragment resembles more an independent molecule as the free valence on H_5 is only 0.13.

The sum of the bond orders of the forming and breaking bonds is close to unity, being between 0.92 and 0.95 for any geometry of TS1 and TS2. The difference between unity and the sum of bond orders appears as free valence on the H atom which is transferred. This shows that for these reactions the principle of conservation of bond order, the underlying assumption of the BEBO method,[28] is not strictly but approximately satisfied (as it was found for simpler reactions earlier[22]). Because of the irregularities found in the case TS3, no firm conclusion can be made concerning reaction 3.

B. Energetics. Detailed energetic data are listed in Table 3 for the BAC-MP4 set of calculations and in Table 4 for the Gaussian-2 calculations. Table 3 shows that the bond additivity and spin projection corrections applied in the BAC-MP4 method are considerable (they may be as large as 50 mhartree (over 30 kcal mol^{-1})); however, they are necessary to get reasonable absolute energies for the species occurring in this study. As expected, the corrections increase with the size of the molecule, and their sum is the largest for the transition structures. The sum of the corrections used in the Gaussian-2 method is also the largest for the transition structures (see Table 4). In order to see how important the various corrections are in determining the accurate barrier heights and reaction energies, in Table 5 we have listed the classical energy differences for the reaction and for activation computed at various ab initio levels. Table 6 shows the differences between the correction terms calculated for the saddle points and for the reactants as well as between

TABLE 3: Energies Used and Obtained in the BAC-MP4 Calculations[a]

species	MP4/ 6-31G**	MP3/ 6-31G**	PMP3/ 6-31G**	BAC correction	spin. proj correction	BAC-corrected MP4	zpe	BAC-MP4	$\Delta H°$ (298) $-\Delta H°$ (0)
H	−0.498 233	−0.498 233	−0.498 233	.000 000	.000 000	−0.498 233	.000 000	−0.498 233	1.481
H_2	−1.164 537	−1.163 141	−1.163 141	.007 024	.000 000	−1.171 561	.010 585	−1.160 977	2.074
H_2O	−76.230 813	−76.225 827	−76.225 827	.034 723	.000 000	−76.265 536	.022 977	−76.242 559	2.372
CH_3	−39.714 719	−39.710 173	−39.711 309	.021 606	.001 137	−39.737 462	.030 971	−39.706 491	2.664
CH_3O	−114.743 907	−114.733 176	−114.734 256	.035 528	.001 080	−114.780 515	.040 274	−114.740 241	2.487
CH_2OH	−114.751 282	−114.739 334	−114.740 270	.046 978	.000 936	−114.799 196	.040 224	−114.785 972	2.684
CH_3OH	−115.410 887	−115.399 081	−115.399 081	.052 442	.000 000	−115.463 329	.055 337	−115.407 992	2.692
TS1	−115.886 952	−115.872 493	−115.875 544	.053 185	.003 051	−115.943 188	.052 531	−115.890 657	3.081
TS2	−115.881 800	−115.866 567	−115.870 464	.049 431	.003 897	−115.935 128	.051 500	−115.883 629	3.077
TS3	−115.853 742	−115.837 107	−115.845 765	.050 477	.008 658	−115.912 877	.053 902	−115.858 975	3.320

[a] All data are given in hartrees except those in the last column which are in kcal $mol.^{-1}$

TABLE 4: Gaussian-2 Energy Data for the Reactants, Products, and Transition Structures[a]

species	E(MP4/ 6-311G**)	ΔE(+)	ΔE(2df)	ΔE(QCI)	ΔE(HLC)	ΔE(ZPE)	E(G1)	ΔE(G2)	E(G2)
H	−0.499 81	0.00	0.00	0.00	−0.19	0.00	−0.500 00	0.00	−0.500 00
H_2	−1.167 72	0.00	0.00	−0.60	−6.14	9.45	−1.165 01	−2.49	−1.166 36
H_2O	−76.276 06	−10.83	−37.39	0.00	−24.56	20.51	−76.328 34	−8.27	−76.332 05
CH_3	−39.730 77	−1.28	−18.06	−1.47	−18.61	27.66	−39.742 53	−5.97	−39.745 08
CH_3O	−114.796 51	−6.71	−57.80	−2.30	−37.03	35.96	−114.864 38	−9.97	−114.867 52
CH_2OH	−114.808 74	−8.30	−58.30	−1.29	−37.03	35.92	−114.877 74	−10.64	−114.881 53
CH_3OH	−115.468 47	−8.87	−59.39	−0.29	−42.98	49.42	−115.530 58	−12.27	−115.534 87
TS1	−115.950 12	−7.93	−58.57	−2.46	−43.17	46.91	−116.015 34	−13.21	−116.020 57
TS2	−115.940 67	−7.22	−58.52	−3.95	−43.17	45.99	−116.007 53	−12.71	−116.012 27
TS3	−115.921 45	−12.59	−57.91	−3.68	−43.17	48.13	−115.990 67	−12.74	−115.995 43

[a] For notation see refs 12 and 14. Energies are given in hartrees, correction terms in mhartrees.

TABLE 5: Classical Energy Differences between the Saddle Point and the Reactants (ΔE_{barr}) and between the Products and the Reactants (ΔE_{react}), Obtained at the Uncorrected ab Initio Levels Used in BAC-MP4 and Gaussian-2 Calculations

	channel 1		channel 2		channel 3	
method	ΔE_{barr}	ΔE_{react}	ΔE_{barr}	ΔE_{react}	ΔE_{barr}	ΔE_{react}
MP4/6-31G**	13.91	−4.20	17.14	0.42	34.75	−22.85
MP2/6-311G**	14.69	−6.60	23.89	4.83	32.46	−21.89
MP4/6-311G**	11.40	−5.13	17.33	2.54	29.39	−24.19
PMP4/6-311G**	9.51	−5.77	14.99	1.81	26.43	−24.91
QCISD(T)/6-311G**	10.04	−6.14	15.03	.91	27.26	−24.93
MP2/6-311+G**	15.32	−6.25	25.08	6.30	30.08	−24.10
MP4/6-311+G**	11.98	−4.78	18.37	3.89	27.05	−26.23
MP2/6-311G**(2df)	15.23	−5.88	24.78	6.32	33.51	−19.16
MP4/6-311G**(2df)	11.92	−4.44	17.88	3.54	30.31	−21.72
MP2/6-311+G**(3df,2p)	15.26	−6.07	25.70	7.67	30.83	−22.61

[a] The units are kcal mol^{-1}.

TABLE 6: The Differences of Correction Terms of the BAC-MP4 and the Gaussian-2 Methods between the Barrier and the Reactants (ΔC_{barr}) as Well as the Products and the Reactants (ΔC_{react}) (in kcal mol^{-1})

	channel 1		channel 2		channel 3	
correction	ΔC_{barr}	ΔC_{react}	ΔC_{barr}	ΔC_{react}	ΔC_{barr}	ΔC_{react}
ΔBAC	0.47	0.98	−1.89	−6.21	−1.23	2.44
Δ(spin corr)	1.91	0.59	2.44	0.68	5.43	0.71
$\Delta E(+)$	.59	.35	1.04	1.35	−2.33	−2.04
ΔE(2df)	.51	.69	.55	1.00	.93	2.47
ΔE(qci)	−1.36	−1.00	−2.29	−1.64	−2.13	−.74
ΔZPE	−1.57	−2.54	−2.15	−2.51	−.80	−.78
ΔG1	9.57	−7.63	14.47	.75	25.04	−25.28
Δ(ΔG2)	−.59	−.53	−.28	−.12	−.30	−1.24

those obtained for the reactants and the products. In Table 7 we present the classical reaction energies and barrier heights obtained with the inclusion of all corrections. It can be seen from Table 5 that the barrier heights and the reaction energies obtained from the MP2 calculations with any basis set are too positive by 5−10 kcal mol^{-1}. The actual barrier heights and reaction energies obtained with different basis sets are within about 2−5 kcal mol^{-1} of each other. By investing more effort into the treatment of electron correlation, more reasonable energies are obtained: as expected, the energy differences are smaller at the MP4 level than at the MP2 level. The change of the barrier heights when going from the MP2 to the MP4 level is about 1−3 kcal mol^{-1} larger than that in the case of the reaction energies. The correction seems not to depend on the type of the basis set. All energy differences calculated at the MP4/6-311G** level are within 1.5 kcal mol^{-1} of the final Gaussian-2 classical energy differences (see Table 7) except for the transition structure of channel 3. The QCISD(T) level brings further corrections to the energy differences, but the changes do not exceed 2.3 kcal mol^{-1}. We also listed the results obtained at the PMP4/6-311G** level. Interestingly, the barrier heights and reaction energies obtained at this level are within 0.9 kcal mol^{-1} of the QCISD(T) energy differences. This indicates that the error in the energy differences due to spin contamination is efficiently removed not only by the expensive QCISD(T) method but by the projection technique which also works well in this set of reactions. The contribution of the additive corrections of the Gaussian-2 method ($\Delta E(+)$, etc.) is relatively small; they actually almost cancel each other (see Table 6). As a result, the final Gaussian-2 classical reaction energies and barrier heights are very close (generally within 1 kcal mol^{-1}) to the values obtained at the MP4/6-311G** level.

The enthalpies of reaction and activation calculated for 0 K and for standard conditions, listed in Table 7, show that channel 3, leading to the formation of CH_3 and H_2O, is the most exothermic one, the formation of CH_2OH channel 1) is slightly exothermic, and the formation of methoxy radicals (channel 2) is almost thermoneutral. This is in agreement with the experimental data:[29−31] the standard experimental enthalpies of reaction are −8.0 kcal mol^{-1} for channel 1, 0.1 kcal mol^{-1} for channel 2, and −27.05 kcal mol^{-1} for channel 3. The agreement between experiment and theory is generally better than 1 kcal mol^{-1}. An exception is channel 2 calculated with the BAC-MP4 method where the difference between the calculated and the experimental reaction enthalpy is 3.4 kcal mol^{-1}, probably due to the least accurate treatment of CH_3O with this method.

The joint analysis of the barrier heights and reaction enthalpies leads to interesting conclusions. One would infer from the reaction energetics that the most exothermic channel has the lowest barrier. The calculations, however, lead to different results. The highest potential barrier proved to be that of channel 3 (V_{bar} = 25.6 and 30.5 kcal mol^{-1} from G-2 and BAC-MP4, respectively), while the lowest barrier belongs to channel 1, i.e., the formation of hydroxymethyl radicals (V_{bar} = 10.6 and 11.3 kcal mol^{-1} from G-2 and BAC-MP4, respectively). Methoxy formation takes place through a medium-sized barrier. A closer examination of the structures, however, indicates that the results obtained for the heights of the barriers are not surprising. The reactions that we compare here do not form a series for which simple structure−reactivity correlations are expected to apply. Instead, here we are faced with three completely different types of reactions: (a) H abstraction from a carbon atom, (b) H abstraction from an oxygen atom, and (c) "OH abstraction." Therefore, it is not surprising that the reaction with the smallest activation energy is not the one which is thermodynamically the most favorable.

TABLE 7: Reaction Energies and Activation Energies (in kcal mol^{-1})

	channel 1		channel 2		channel 3	
energy difference	BAC-MP4	G2	BAC-MP4	G-2	BAC-MP4	G-2
$\Delta_f H°_{298}$	−8.03	−7.58	3.53	1.01	−26.01	−25.65
$\Delta_f H_{00}$	−8.61	−8.17	3.14	0.63	−26.87	−26.51
V_{cl}(reaction)	−6.07	−5.63	3.65	3.14	−26.09	−25.73
$\Delta H°_{298}$(TS)	8.68	7.89	13.08	13.09	28.80	23.90
ΔH_{00}	9.77	8.98	14.18	14.19	29.65	24.76
V_{cl}(TS)	11.34	10.55	16.33	16.34	30.45	25.56

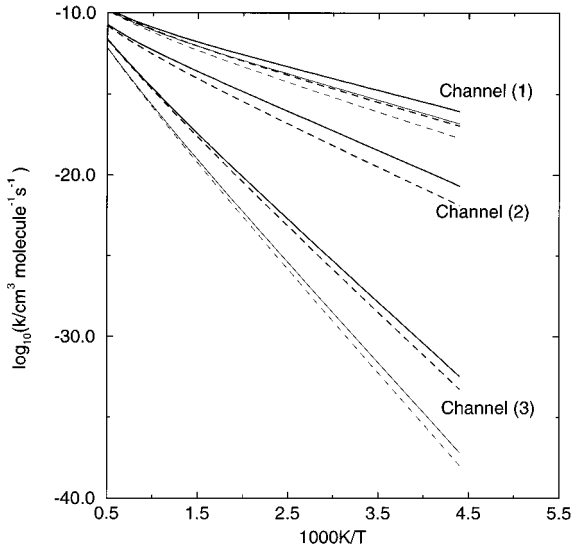

Figure 2. Rate coefficients for reactions 1, 2, and 3 obtained from conventional transition state theory calculations using ab initio barrier heights and vibrational frequencies: Gaussian-2 (thick lines), and BAC-MP4 data (thin lines), without (dashed lines) and with (continuous lines) inclusion of tunneling correction.

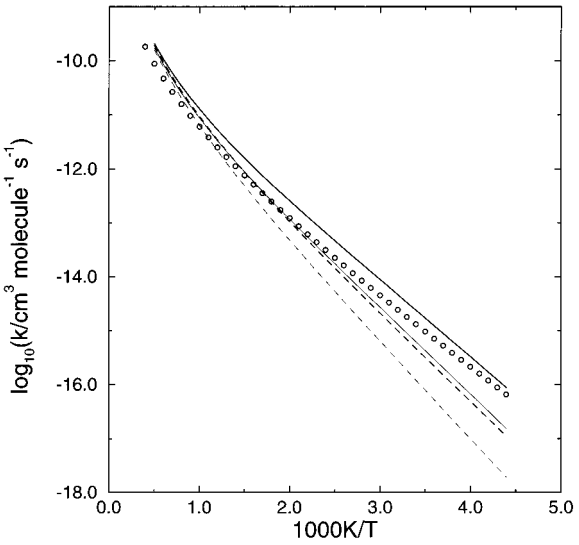

Figure 3. Comparison of experimental and theoretical results on the overall rate coefficient: Tsang's recommendation[2] (○ ○ ○) and Gaussian-2 (thick lines) and BAC-MP4 data (thin lines), without (dashed lines) and with (continuous lines) inclusion of tunneling correction.

The results obtained with the BAC-MP4 and Gaussian-2 methods compare well with each other. The difference in the calculated standard reaction heats is about 0.5, 2.5, and 0.4 kcal mol^{-1} in the three channels, respectively. The classical barrier heights differ by about 0.8, 0.0, and 4.9 kcal mol^{-1}, respectively. The accuracy of the Gaussian-2 method is about 2 kcal mol^{-1} for stable molecules;[12] the estimated error of the BAC-MP4 calculations varies from molecule to molecule,[9,11] but it is generally also about 1−2 kcal mol^{-1}. In light of this, the barrier heights of channels 1 and 2 are obtained with good accuracy, in particular that of channel 2. The accuracy of the experimental activation energy determined for a system which lends itself to a reliable measurement is rarely better than 1 kcal mol^{-1}, so that the agreement of the theoretical results for channel 1 should be considered very good. The accuracy of the barrier height of channel 2 is still reasonable. The larger difference between the BAC-MP4 and Gaussian-2 barrier heights for channel 3 falls outside of the optimum range of accuracy. Fortunately, among the three channels considered, this is the least important process from the point of view of reaction kinetics, since the barrier height is significantly larger than that of the other two competing channels. As a result, even though the barrier height of channel 3 is not known very accurately, one expects that the overall reaction is dominated by the rate of the hydroxymethyl- and methoxy-forming reactions and the formation of methyl radical and water is negligible.

C. Rate Coefficients. Using the ab initio data, one can determine the rate coefficients corresponding to each channel. The sum of these rate coefficients gives the overall rate of consumption of methanol, which can be compared with experimental data found in the literature. With the rate coefficients of the three channels known, assessment of their relative importance becomes possible.

The Arrhenius plot of the rate coefficients of the three channels is presented in Figure 2. As expected, the rate coefficient for channel 1 is much larger at any temperature up to 2000 K than those of the other two channels. As the barrier heights obtained with the BAC-MP4 and the Gaussian-2 methods are very similar for channel 2, the rate coefficients calculated for channel 2 using the two methods are essentially identical. For channel 1 lower rate coefficients can be obtained from the BAC-MP4 energetics than from the G-2 data. The difference is a factor of 4.35 at 300 K and 1.32 at 1500 K. As expected, the most significant difference occurs for channel 3 where the difference in the barrier heights is the largest. Namely, the BAC-MP4 rate coefficient is smaller than that derived from the Gaussian-2 data by a factor of 3400 at 300 K and by a factor of 5.6 at 1500 K. In the discussions that follow, we use the Gaussian-2 data. The conclusions are, however, very similar if the BAC-MP4 data are used.

A comparison of the experimental and theoretical overall rate coefficients is given in Figure 3. There is a very good agreement with the recommendation of Tsang[2] all over the temperature range studied. The rate coefficients calculated using the Gaussian-2 energetic data and tunneling correction are higher than the recommendation, but the difference is less than a factor of 2 all over the temperature range 300−2000 K. The BAC-MP4 results lead to smaller rate coefficients than those calculated from Tsang's recommendation, but the difference is not larger than a factor of 3 even at 300 K where the difference is the largest. The empirical rate equation of

$$k = BT^n \exp(-H/T)$$

was fit to the theoretical rate coefficients. The fitting parameters obtained from the Gaussian-2 + tunneling calculations are $B = (1.57 \pm 0.56) \times 10^{-15}$ cm^3 molecule^{-1} s^{-1}, $n = 1.70 \pm 0.05$, and $H = 2735 \pm 23$ K. (Note that the fit was made between 300 and 2000 K with the Marquardt algorithm; the parameters B and n are highly correlated.) It follows from the large value obtained for the fitting parameter n that the Arrhenius activation energy increases significantly with increasing temperature which corresponds to a concave Arrhenius plot. The actual activation energies calculated by numerical differentiation of the log(k) vs 1/T data, shown in Figure 4 for the overall reaction, increase with increasing T. The rate of increase is similar for each reaction channel.

The available experimental rate coefficient data were obtained in two different temperature regimes: direct measurements were performed at low temperatures (298−640 K), while high-temperature data (at $T > 1000$ K) were derived from flame experiments and shock tube measurements (see the excellent review by Grotheer et al.[3]). The two sets of measurements are hard to reconcile. The low-temperature rate coefficients are

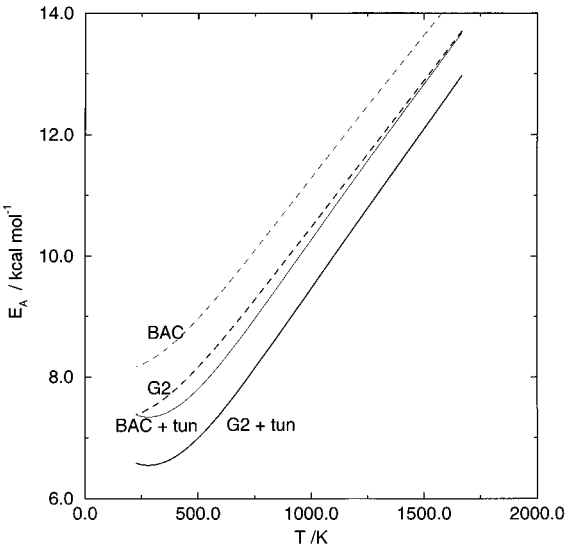

Figure 4. Temperature dependence of the Arrhenius activation energy for the overall reaction, calculated by numerical differentiation of the curves in Figure 3: Gaussian-2 (thick lines) and BAC-MP4 data (thin lines), without (dashed lines) and with (continuous lines) inclusion of tunneling correction.

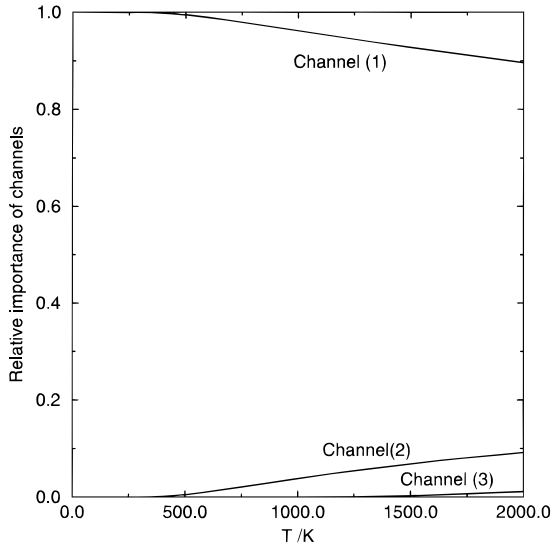

Figure 5. The contribution of channels 1−3 to the overall reaction as a function of the temperature (Gaussian-2 data with inclusion of tunneling correction).

generally lower than what would be expected from the extrapolation of the high-temperature data. This may indicate that the activation energies suggested for the high temperatures are too low. Comparison with the present theoretical results supports this opinion.

The relative importance of the individual channels is the key factor influencing the formation of the different radicals in the reaction of H atoms with methanol and determining the role that these reactions play in combustion systems. None of the experimental studies addressed this question so far because of the difficulties associated with measuring different reactive radicals simultaneously. Theoretical calculations complementing the experiments can fill in this gap. The calculated branching ratio, i.e., the ratio of the rate coefficient of a particular channel to the sum of the rate coefficients of all three channels, is displayed as a function of temperature in Figure 5. Channel 1, i.e., H atom abstraction from the methyl group, dominates the reaction in the entire chemically interesting temperature range. With increasing temperature, the contribution of the processes with higher activation energies increases a little: channel 2 contributes to the overall rate by about 4% at about 1000 K, but its participation remains less than 10% even at 2000 K. Channel 3 can hardly be observed even at 2000 K. On the basis of these results one can conclude that in most modeling studies of methanol combustion it is satisfactory to consider the reaction $H + CH_3OH$ as a single-channel process leading to the formation of hydroxymethyl radicals and H_2.

TABLE 8: The Kinetic Isotope Effect $k_{substituted}/k_{unsubstituted}$ for Various Isotopic Substitutions of the Reactant Methanol[a]

		temperature		
reactant	product	2000 K	1000 K	300 K
		Channel 1		
CH_2DOH	CH_2OH	0.471	0.383	0.129
CH_2DOH	CHDOH	0.616	0.610	0.576
CH_3OD	CH_2OD	0.623	0.624	0.632
CD_3OH	CD_2OH	0.469	0.379	0.121
		Channel 2		
CH_2DOH	CH_2DO	0.619	0.617	0.608
CH_3OD	CH_3O	0.449	0.345	0.093
CD_3OH	CD_3O	0.622	0.623	0.621
		Channel 3		
CH_2DOH	CH_2D	0.618	0.597	0.519
CH_3OD	CH_3	0.616	0.611	0.583
CD_3OH	CD_3	0.599	0.578	0.411

[a] For channel 1 the isotope effect is calculated on a per H atom basis.

D. Isotope Effects. Isotope substitution often helps to establish the mechanism of a reaction. In the present case, it might be possible to identify the main channel of the reaction from the measurement of the isotope effect on the overall rate coefficient of methanol consumption, provided that the reaction is dominated by a single channel. In order to help to design such experiments, we calculated the isotope effects for reactions of methanol molecules in which one or more of the H atoms were substituted by deuterium. The reactions of H atoms with CH_2DOH, CH_3OD, and CD_3OH were considered. The isotope effect calculated at various temperatures for the three reaction channels are presented in Table 8. In the calculation of the rate coefficients for the reactions with different substituted reactants, the same classical barrier heights were used (those obtained from the Gaussian-2 calculations) but the vibrational frequencies were recalculated from the force field of each species.

A quick survey of the data shows that the secondary isotope effect caused by deuterium substitution is in most cases around $k_{substituted}/k_{unsubstituted} = 0.6$. This indicates that an unequivocal identification of the dominant channel is only possible if the reduction of the rate is extremely large. The isotope effect in the case of channel 3 is insensitive to the site of deuterium substitution. The rate coefficient for channel 1, as expected, decreases significantly if the hydrogens on the carbon atom are replaced by deuterium, while for channel 2 a large isotope effect is observed if the hydrogen of the OH group is substituted.

The reaction with CH_2DOH is not very informative: the isotope effect for the overall reaction (the weighted sum of the data in the top two lines of the table) would be 0.567, 0.534, and 0.427 at 2000, 1000, and 300 K, respectively, if channel 1 dominates, and these data are too close to the values characterizing channel 2 (which are around 0.61 at each temperature) and channel 3 (which change between 0.61 and 0.51). Using CH_3OD as a reactant, an isotope effect of about 0.6 would not allow one to conclude if channel 1 or channel 3 dominates. If, however, the measured isotope effect is below 0.45 at 2000 K and around 0.35 at 1000 K, the reaction probably takes place through channel 2.

Similar conclusions can be drawn from the investigation of the data of CD_3OH as reactant. With this reactant, in principle, one can distinguish channel 1 from the other two. It seems to us, however, that it is difficult to obtain experimentally definitive answers from the study of the isotope effect. Assuming that a rate coefficient can be measured with an accuracy of 50%, the difference between the isotope effects of 0.62 to 0.35 (as in the case of CH_3OD at 1000 K) or 0.62 to 0.3 (as in the case of CD_3OH at 1000 K) seems to be too small to distinguish between the various channels. Thus, we conclude that determination of the isotope effect for the overall reaction seems not to be a conclusive way for identifying the mechanism of the reaction.

IV. Conclusion

The calculation of the rate coefficients for the three channels of the H + CH_3OH reaction using two ab initio methods shows that channel 1, i.e., the formation of hydroxymethyl radicals, is the dominant route. More than 96% of methanol reacting with H atoms is converted into CH_2OH at 1000 K, about 93% at 1500 K, and 90% at 2000 K. Formation of methoxy radicals via channel 2 contributes to the overall rate by about 4%, 7%, and 9% at these temperatures, respectively. Formation of methyl radicals in channel 3 becomes appreciable only above 2000 K. The actual values of the overall rate coefficient and its temperature dependence is in very good agreement with Tsang's recommendation.

The barrier heights obtained with the Gaussian-2 and the BAC-MP4 methods are in very good agreement for two channels, i.e., for hydroxymethyl and methoxy formation. Taking into account that both the Gaussian-2 and the BAC-MP4 methods were developed on the basis of large sets of stable compounds, the agreement obtained in the calculation of the relative energies of the transition structures (the barrier heights) by the two methods provides mutual support for the future application of both methods in the calculation of barrier heights. The relatively larger difference in the calculated barrier heights for channel 3 has no important consequences concerning the kinetics since this channel is essentially unimportant at the temperatures of methanol combustion.

Acknowledgment. The ab initio calculations were performed with Gaussian 92 on IBM 3090 (CIRCÉ) and RISC/6000 (Univ. Nancy) computers in France. G.L. is grateful to Professor J.-L. Rivail and Dr. J. G. Ángyán for their hospitality during his visit in Nancy. The research reported here was supported by the Hungarian National Research Fund (Grant T15819) and by the E.C. project entitled "Chemical kinetic studies of combustion related atmospheric pollution processes" (contract no. CIPA-CT93-0163).

References and Notes

(1) (a) Marshall, E. *Science* **1989**, *246*, 199. (b) Morton, L.; Hunter, N.; Gesser, H. *Chem. Ind.* **1990**, 457.
(2) Tsang, W. *J. Phys. Chem. Ref. Data* **1987**, *16*, 471.
(3) Grotheer, H.-H.; Kelm, S.; Driver, H. S. T.; Hutcheon, R. J.; Lockett, R. D.; Robertson, G. N. *Ber. Bunsen-Ges. Phys. Chem.* **1992**, *96*, 1360.
(4) Aders, W.-K.; Wagner, H. G. *Z. Phys. Chem.* **1971**, *74*, 224.
(5) Aronowitz, D.; Naegeli, D. W.; Glassman, I. *J. Phys. Chem.* **1977**, *81*, 2555.
(6) Hoyermann, K.; Sievert, R.; Wagner, H. G. *Ber. Bunsen-Ges. Phys. Chem.* **1981**, *5*, 149.
(7) Spindler, K.; Wagner, H. G. *Ber. Bunsen-Ges. Phys. Chem.* **1982**, *6*, 2.
(8) Warnatz, J. In *Combustion Chemistry*; Gardiner, W. C., Jr., Ed.; Springer: New York, 1984.
(9) Melius, C. F. In *Chemistry and Physics of Energetic Materials*; Bulusu, S. N., Ed.; Kluwer Academic Publishers: Dordrecht, The Netherlands, 1990.
(10) Ho, P.; Melius, C. F. *J. Phys. Chem.* **1995**, *99*, 2166.
(11) Allendorf, M. D.; Melius, C. F. *J. Phys. Chem.* **1993**, *97*, 720.
(12) Curtiss, L. A.; Raghavachari, K.; Trucks, G. W.; Pople, J. A. *J. Chem. Phys.* **1991**, *94*, 7221.
(13) Curtiss, L. A.; Carpenter, J. E.; Raghavachari, K.; Pople, J. A. *J. Chem. Phys.* **1992**, *96*, 9030.
(14) Curtiss, L. A.; Raghavachari, K.; Pople, J. A. *J. Chem. Phys.* **1993**, *98*, 1293.
(15) Durant, J. L.; Rohlfing, C. M. *J. Chem. Phys.* **1993**, *98*, 8031.
(16) Frisch, M. J.; Trucks, G. W.; Head-Gordon, M.; Gill, P. M. W.; Wong, M. W.; Foresman, J. B.; Johnson, B. G.; Schlegel, H. B.; Robb, M. A.; Replogle, E. S.; Gomperts, R.; Andres, J. L.; Raghavachari, K.; Binkley, J. S.; Gonzalez, C.; Martin, R. L.; Fox, D. J.; Defrees, D. J.; Baker, J.; Stewart, J. J. P.; Pople, J. A. *Gaussian 92*, Revision C; Gaussian, Inc.: Pittsburgh, PA, 1992.
(17) Dupuis, M.; Farazdel, A.; Karna, S. P.; Maluendes, S. A. HONDO 8.0. In *Modern Techniques in Computational* Chemistry*: MOTECC-90*; Clement, E., Ed.; ESCOM: Leiden, The Netherlands, 1990; p 277.
(18) Smith, I. W. M. *Kinetics and Dynamics of Elementary Gas Reactions*; Butterworths: London, 1980.
(19) Laidler, K. J. *Theories of Chemical Reaction Rates*; McGraw-Hill: New York, 1969.
(20) Mayer, I. *Chem. Phys. Lett.* **1983**, *97*, 210; **1985**, *117*, 396 (addendum).
(21) Mayer, I. *Int. J. Quantum Chem.* **1984**, *26*, 151.
(22) Lendvay, G. *J. Phys. Chem.* **1989**, *93*, 4422.
(23) Lendvay, G. *J. Phys. Chem.* **1994**, *98*, 609.
(24) (a) Ángyán, J. G. *J. Mol. Struct.* **1989**, *168*, 61. (b) Ángyán, J. G.; Poirier, R. A.; Kucsman, Á.; Csizmadia, I. G. *J. Am. Chem. Soc.* **1987**, *109*, 2237.
(25) Lendvay, G. *J. Mol. Struct.* **1988**, *167*, 331.
(26) Somogyi, Á.; Tamás, J. *J. Phys. Chem.* **1990**, *94*, 5554.
(27) Lendvay, G. *Chem. Phys. Lett.* **1991**, *181*, 88.
(28) Johnston, H. S. *Gas Phase Reaction Rate Theory*; Ronald Press: New York, 1966.
(29) Dóbé, S.; Bérces, T.; Turányi, T.; Márta, F.; Grussdorf, J.; Temps, F.; Wagner, H. G. *J. Phys. Chem.*, in press.
(30) *TRC Thermodynamic Tables—Non Hydrocarbons*; The Texas A&M University System: College Station, TX, December 31, 1986 (data for CH_3OH).
(31) Chase, M. W., Jr.; Davis, C. A.; Downey, J. R., Jr.; Frurie, D. J.; McDonald, R. A.; Syverud, A. N. *JANAF Thermochemical Tables*, Third Edition. *J. Phys. Chem. Ref. Data* **1985**, *14*, (Suppl. 1).